Some mathematical appreciations in the physical sciences

JOHN MAHONY

Introduction

According to reports in the media, there is a dearth of practical examples that students of mathematics en route to their qualification can feast upon, at either sixth form level or an undergraduate level. Despite these alleged shortages, it is this author's opinion that there are numerous examples that can be drawn from the literature and it is the purpose of this article to address the issue by providing examples from the realms of antenna reflector theory and the use therein of conic sections. Some students will be familiar with conic sections and others might not, but the numerous instances of their manifestation in the real world would suggest that they are a force to be reckoned with, and this is certainly true from a mathematical perspective.

Here we will discuss the geometry and associated mathematics of conic sections, so that the reader can appreciate just how they can be used in the design of reflector antennas, or dishes as they are sometimes called. In the first instance, this will be done for the geometry of a single-reflector system and then the process will be carried over to address two different dual-reflector system scenarios that, to use the nomenclature of telescope design, are known as the classical Cassegrain type and the classical Gregorian type. Finally, it will be shown how the classical concept can be modified to produce a refined offset reflector geometry that circumvents problems associated with the classical design.

Reflector geometries

(a) *Single reflector systems*

Readers will most likely might be aware of the shape of the conic section called a parabola. It has one focal point on its axis of symmetry and for reasons to be explained later it is the building block for reflector antenna systems. The interest here is in a centre-fed paraboloidal system, that is to say, the reflector shape is that of a parabola rotated about its axis to produce a structure in three-dimensions. A small horn antenna pointing towards the centre of the paraboloid is located at the focus and it serves to illuminate the dish with energy in the RF (Radio Frequency) spectrum. Such configurations are commonplace, and a trip outside to look at nearby rooftops would likely reveal examples in the form of satellite receiving dishes, although not all would be centre-fed systems, but would have instead a feed located at a focus pointing at an offset portion of a paraboloid. Because of symmetry in centre fed systems, it is fruitful to consider a two-dimensional geometry for them, such as that shown in Figure 1.

https://doi.org/10.1017/mag.2021.3 Published online by Cambridge University Press

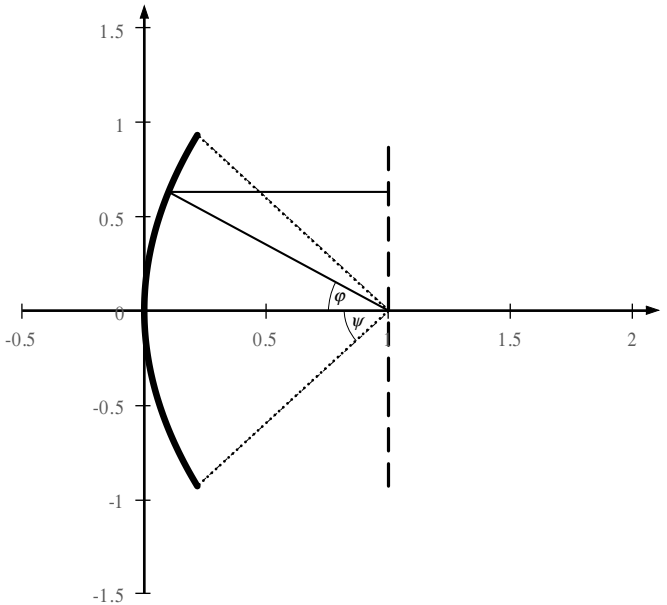


FIGURE 1: A typical two-dimensional schematic of a paraboloid and its focal plane
x-axis horizontal: y-axis vertical
(Dimensions are normalised with respect to the focal length)

In this figure, a point source feed is located at the focus (unit distance from the origin) and it radiates a bundle of rays of energy within a cone of half-angle ψ to illuminate the dish. A typical ray that subtends an acute angle φ with the reflector axis is also shown in the figure. In the usual xy-coordinate system, the shape of the parabola can be described by the equation $y^2 = 4fx$, where f denotes the focal length (in Figure 1, it is unity). The coordinates of a point on the reflector where the typical incident ray impinges is given by $x = ft^2$ and $y = 2ft$, where $t = \tan\frac{1}{2}\phi$. It is left as an exercise for the reader to show that if a typical incident ray is reflected according to Snell's law (the angle of incidence with respect to the normal is equal to the angle of reflection), then the reflected ray is parallel to the axis of the parabola. Moreover, the distance from the focal point to the point of reflection is $ft^2 + f$ and the distance thereafter to the focal plane can be shown to be $f - ft^2$, so that the sum of these two distances is simply $2f$, which is independent of φ. Thus all incident rays are collimated on reflection (that is to say they are all parallel) and their path lengths from the focus to the focal plane are the same. Since the phase of the energy associated with a given ray is dependent on its path length, this shows that there is no phase distortion between rays by the time the focal plane is reached. It is these properties of the parabola that make it so appealing to telecommunication engineers (a spherical wave front from the feed has been converted to a plane wave front). It is pertinent to point out at this juncture

https://doi.org/10.1017/mag.2021.3 Published online by Cambridge University Press

that edge rays from the illuminating cone in this scenario form a circle in the focal plane. The region within this bounding circle is known as a projected aperture and it is an important concept for antenna engineers. Using the above expressions for the cartesian coordinates of a point on the parabola, it is a straightforward matter to plot it on a spreadsheet for $\varphi\ (-\psi \leqslant \varphi \leqslant \psi)$, and obtain a result like that shown in Figure 1.

Another important parameter of interest to antenna engineers is the ratio f/d where d denotes the diameter of the projected aperture. This is an important term, because if it is chosen wisely it can help optimise reflector antenna performance. It is hoped to make this the subject of a future note. Moreover, it can be shown that the ray angle $\psi\ (0 \leqslant \psi < \frac{1}{2}\pi)$ subtended at the reflector rim is related to this ratio via the equation

$$\frac{f}{d} = \frac{0.25}{\tan\frac{1}{2}\psi}. \tag{1}$$

(b) *Dual reflector systems*

Cassegrain type: Perhaps the most common form of a dual reflector system is one involving a paraboloidal main reflector and a hyperboloidal sub-reflector, the former being concave with respect to the feed point and the latter being convex. Systems like this are usually employed when there are constraints on the space available to house a single reflector system, such as in the nose cone of an aircraft. One such configuration is pictured in Figure 2. Such configurations are to be found also on satellite ground stations for pretty much the same reasons – economy of space.



FIGURE 2: A Panavia Tornado F3 fighter plane with its Radar system alongside on a trolley
(©Ad Meskens/Wikimedia Commons)

https://doi.org/10.1017/mag.2021.3 Published online by Cambridge University Press

This photograph shows, in particular, the front end of the Tornado F3 Cassegrain Radar system looking roughly like the frustum of a right circular cone with a protective cover. Under this cover is a composite dual reflector unit comprising a paraboloidal main reflector (at the rear) and a smaller hyperboloidal sub-reflector (at the front). Also on the trolley behind this composite unit are supporting components and other system parts. For the bigger picture, the interested reader should go to [1].

There is rotational symmetry about an axis and it will suffice here to display a two-dimensional schematic for this classical Cassegrain system, such as that shown in Figure 3, along with other information.

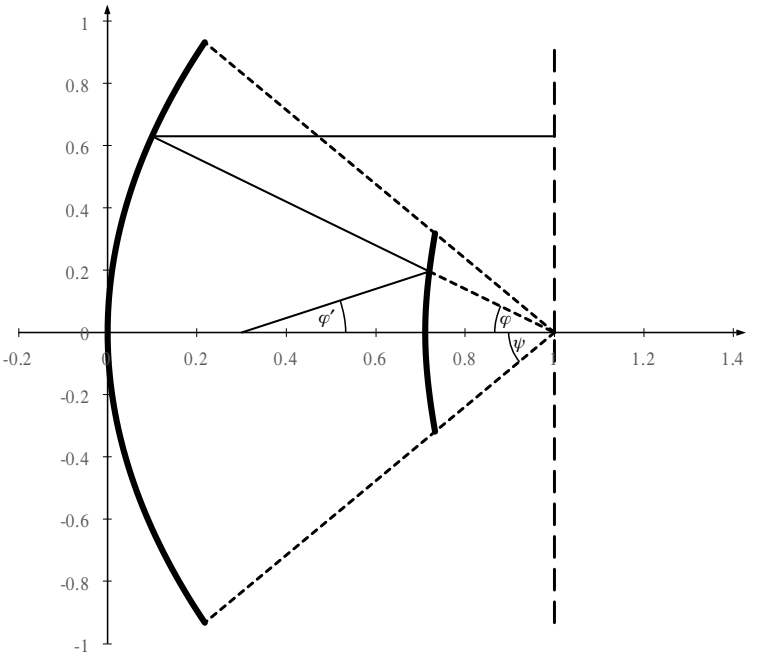


FIGURE 3: A two-dimensional schematic for a classical Cassegrain dual reflector system showing typical ray paths and angles of interest when $\gamma = 80°$, $d' = 0.3$ and $\psi = 50°$.
Real feed point is at the hyperbola focus between reflectors.
Virtual feed point is at parabola focus (the other hyperbola focus).

In the Figure, the focus of the parabolic main reflector is at a distance unity along the horizontal axis from the origin. This is known as a virtual focus, and it is also one of the focal points of the hyperbolic sub-reflector. The other focal point for the hyperbola is shown on the horizontal axis at some distance, d' say, from the origin (here $d' = 0.3$). It is the feed point for the dual reflector system, and it is the real focus. The eccentricity of the hyperbola in the Figure is $e = \sec\gamma$, where $\gamma = 80°$. Also shown is a ray emanating from the real focus. It is reflected from a point on the hyperbola and travels to a reflection point on the parabola along a path as if it had been

https://doi.org/10.1017/mag.2021.3 Published online by Cambridge University Press

a direct ray from the virtual focus through the point of reflection on the hyperbola. It is left as an exercise for the reader to establish that the direct ray from the virtual focus in this fashion does indeed make an angle with the normal at the reflection point that is the same as the angle made similarly by the ray from the real focus, in accordance with what is to be expected from Snell's law. Rays from the real feed position in this figure are constrained on reflection at the hyperbola to lie within an energy cone (dotted lines) emanating from the virtual feed point. The virtual focus lies in the projected aperture plane (dashed line).

As before, a point on the parabola can be characterised by the parametric representation $x = ft^2$ and $y = 2ft$, where $t = \tan\frac{1}{2}\varphi$ and where the origin of the coordinate system is the parabola's vertex. Also, in the usual notation, a point of reflection on the hyperbola can be represented parametrically by $x = a\sec\theta$ and $y = b\tan\theta$, referenced to a parallel cartesian axes system centred midway between the real focus and the virtual focus. The distance between these focal points is $2ae$. Since $e = \sec\gamma$, it follows that $b = a\tan\gamma$. Thus, with reference to the parabola's coordinate system, the reflection point on the hyperbola is $x = a\sec\theta + ae + d'$ and $y = b\tan\theta$. It is a simple matter to plot the parabola for $-\psi \leqslant \varphi \leqslant \psi$ in a rectangular cartesian coordinate system. Similarly, in order to plot the hyperbola an expression for the parameter θ in terms of φ will be required. Moreover, it will be appropriate to obtain also at this juncture an expression for φ' in terms of known parameters, for use later when discussing the concept of the equivalent parabola. This can be obtained by first obtaining two trigonometric expressions from the Figure:

$$\tan\varphi = \frac{b\tan\theta}{ae - a\sec\theta} \tag{2}$$

and

$$\tan\varphi' = \frac{b\tan\theta}{ae + a\sec\theta}. \tag{3}$$

Then, b can be replaced by $a\tan\gamma$ to produce the following expressions

$$\tan\varphi = \frac{\sin\gamma\sin\theta}{\cos\theta - \cos\gamma} \tag{4}$$

and

$$\tan\varphi' = \frac{\sin\gamma\sin\theta}{\cos\theta + \cos\gamma} \tag{5}$$

respectively.

https://doi.org/10.1017/mag.2021.3 Published online by Cambridge University Press

The usual half-angle formula for terms involving θ can be employed in these expressions to obtain quadratics in $\tan\frac{1}{2}\theta$ that can be solved to produce roots of interest, in the form

$$\theta = 2\tan^{-1}\left(\tan\tfrac{1}{2}\gamma\,\tan\tfrac{1}{2}\varphi\right) \tag{6}$$

and

$$\varphi' = 2\tan^{-1}\left(\tan\tfrac{1}{2}\gamma\,\tan\tfrac{1}{2}\theta\right),$$

from which it follows that

$$\varphi' = 2\tan^{-1}\left(\tan^2\tfrac{1}{2}\gamma\,\tan\tfrac{1}{2}\varphi\right). \tag{7}$$

In addition, the hyperbola parameter a required in the plotting procedure can be related to the parabola focal length $f\,(=1)$, the hyperbola eccentricity e and the real feed offset distance d' via the equation $a = 0.5(f - d')\cos\gamma$. It is left as an exercise for the reader to carry out the ensuing calculations and obtain a plot such as that of Figure 3 following input values for γ, d' and ψ.

As with the parabola in the single reflector system (see above), it can be shown that the overall ray path length to the projected aperture for all rays in this system is the same. To appreciate this, denote the concomitant ray path lengths by d_1, d_2 and d_3, where the first is the path length from the real feed point to the point of reflection on the hyperbolic sub-reflector, the second is the path length from this point to the point of reflection on the parabolic main reflector and the last is the distance from the reflection point on the main reflector to the projected aperture. Their sum is $(d_1 + d_2 + d_3)$. Moreover, if d_1' denotes the distance from the virtual feed point to the point of reflection on the hyperbolic sub-reflector, then $(d_1' + d_2 + d_3)$ is simply the distance described in the previous section for the ray path length in a single parabolic reflector system, that is, twice the focal length. Thus $(d_1' + d_2 + d_3) = 2f$, and the focal length of the parabola here is unity. Finally, another well-known property of the hyperbola which, with reference to Figure 3, is that $d_1 - d_1' = 2a$. The reader might care to establish this as well, either by methods of pure geometry [2] or by methods of algebraic trigonometry coupled with coordinate geometry. Thus, combining these two results, it follows that $d_1 + d_2 + d_3 = 2f + 2a$, which is the same for all ray path lengths. As with the single reflector system, there is no phase distortion across the projected aperture in this dual reflector system and rays reflected from the parabola are therefore collimated.

Gregorian type: Just as the classical Cassegrain dual reflector system comprises a paraboloidal main reflector, so too does the classical Gregorian system. However, the sub-reflector is different, being a portion of an ellipsoid. Again, because of rotational symmetry it will suffice to consider only a two-dimensional schematic such as that shown in Figure 4.

https://doi.org/10.1017/mag.2021.3 Published online by Cambridge University Press

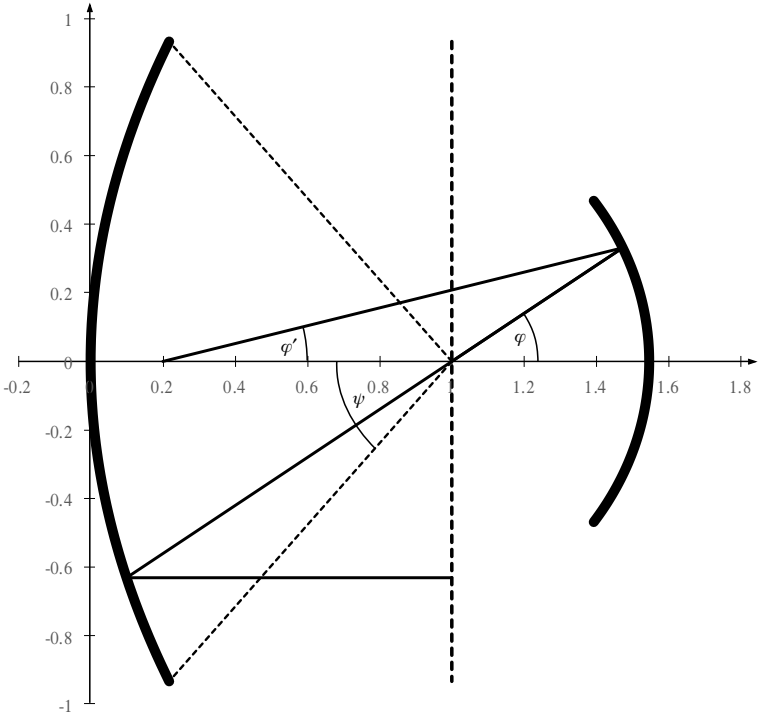


FIGURE 4: A two-dimensional schematic for a classical Gregorian dual reflector system showing a typical ray path and angles of interest when $\gamma = 65$, $d' = 0.2$ and $\psi = 50°$.
Real feed point is at the first ellipse focus (on the left).
Virtual feed point is at the second ellipse focus (on the right); this is also the parabola focus.

With reference to the Figure, a feed is positioned at the first focus of the ellipse, where $d' = 0.2$, and a typical ray from it impinges on an upper-half portion of the ellipse where it is reflected according to Snell's law to pass back through the second focus (at a distance unity along the horizontal axis) and on to the lower-half of the parabolic reflector where it is reflected again in accordance with the principles of reflection from a parabola. There are several issues for the reader to understand at this point and they can be appreciated by first referencing a typical point on the sub-reflector in the usual notation. Specifically, with reference to a rectangular cartesian coordinate system centred at a point midway between the two foci, the point on the sub-reflector will have coordinates given by $x = a\cos\theta$ and $y = b\sin\theta$. The eccentricity of the ellipse is less than unity and will therefore be denoted by $e\,(=\cos\gamma)$. Then it follows that the parameter b equals $a\sin\gamma$. The interested reader might care to prove that the normal at such a point bisects the angle subtended there by the two foci (in accordance with Snell's law). This can be shown using methods of algebraic

https://doi.org/10.1017/mag.2021.3 Published online by Cambridge University Press

trigonometry to determine angles between lines etc., or it can be deduced using pure geometry as described in [2]. Finally, it is important to appreciate also for this classical Gregorian configuration that the path length of a typical ray from the feed to a point in the projected aperture is the same for all rays. It is left as an exercise for the reader to show that it is simply $2a + 2f$. Rays reflected from the parabola are of course collimated and there is no phase distortion across the projected aperture.

Again, with reference to the figure, a point on the parabola can be characterised in the usual way by the parametric representation $x = ft^2$ and $y = -2ft$, where $t = \tan\frac{1}{2}\varphi$ and where the origin of the coordinate system is the parabola's vertex. Also, with reference to the parabola's xy-system, the reflection point on the ellipse is $x = a\cos\theta + ae + d'$ and $y = b\sin\theta$. It is a simple matter to obtain a spreadsheet plot of the parabola in this system for $-\psi \leqslant \varphi \leqslant \psi$. Similarly, in order to plot the ellipse, an expression for the parameter θ in terms of φ will be required, as in the Cassegrain case above. It is necessary to establish formulae akin to those for the Cassegrain case, namely equations paralleling those given in (2) and (3). It can be seen from the figure that the analogous equations in this case are

$$\tan\varphi = \frac{b\sin\theta}{a\cos\theta - ae}$$

and

$$\tan\varphi' = \frac{b\sin\theta}{a\cos\theta + ae}$$

respectively. However, since $e = \cos\gamma$ and $b = a\sin\gamma$, it follows that (4) and (5) apply also to this scenario, as then must (6) and (7), provided the angles and eccentricity terms there are interpreted accordingly. To complete the plotting exercise, it will be necessary to relate the ellipse parameter a to the ellipse eccentricity, the feed offset distance and the parabola length via the equation $a = \dfrac{0.5(f - d')}{\cos\gamma}$.

(c) *Equivalent parabola*

With reference to the Cassegrain system of Figure 3, an illustration of the equivalent parabola is shown in Figure 5. This concept was introduced in [3] to facilitate ease of analysis of the electrical performance in centre fed dual reflector systems. In this figure the dotted-line parabola is the equivalent one. It has the same projected aperture as the original parabola, but its focus is now at the real feed position of the dual reflector system. Typical ray paths are shown both for the original dual system and for the equivalent system, so that one can appreciate how they interconnect. In the absence of the hyperbolic sub-reflector, a ray from the virtual feed point will be reflected off the main parabola to a reflection point on the equivalent parabola, whereupon it is redirected to the real feed point of the dual system, and vice versa, with a crossover point that would lie on the sub-reflector

https://doi.org/10.1017/mag.2021.3 Published online by Cambridge University Press

when present. The angles φ' and φ in Figure 3 apply in this case and their values at the reflector edges are the angles ψ' (at the edge of the equivalent parabola) and ψ (at the edge of the main reflector edge), respectively. In order to plot the equivalent parabola in the same coordinate system as the original parabola, it will be necessary to exploit some of the above relationships. From the configuration in Figure 5, the x and y coordinates of a typical point on the equivalent parabola (ep) can be written in the form $x_{ep} = d' + f' - f't'^2$ and $y_{ep} = 2f't'$, where $t = \tan\frac{1}{2}\varphi'$ and f' denotes the focal length of the equivalent parabola. Using (1) and its counterpart for the equivalent parabola, f' can be related to f by the equation

$$f' = f\frac{\tan\frac{1}{2}\varphi}{\tan\frac{1}{2}\varphi'}.$$

This will be the same for all pairings of φ and φ', and to plot the ensuing equivalent parabola for values of φ in the range $(-\psi \leqslant \varphi \leqslant \psi)$ one must establish first a relationship between them. This is provided by (7), where φ' is given explicitly in terms of φ and γ. Values for φ and φ' can be employed now to determine corresponding values for f' and t', and hence the corresponding coordinates of the equivalent parabola.

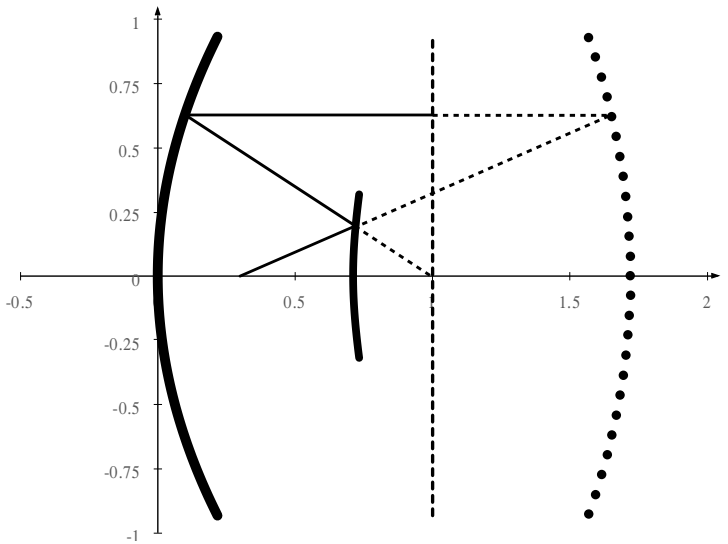


FIGURE 5: The equivalent parabola concept pertaining to the Cassegrain case of Figure 3

Having discussed the concept of the equivalent parabola in the context of the Cassegrain system, it is not too difficult to repeat the exercise in respect of the Gregorian system shown in Figure 4. The fine details are left as an exercise for the reader, but the end result of a plot should be as shown in the Figure 6.

https://doi.org/10.1017/mag.2021.3 Published online by Cambridge University Press

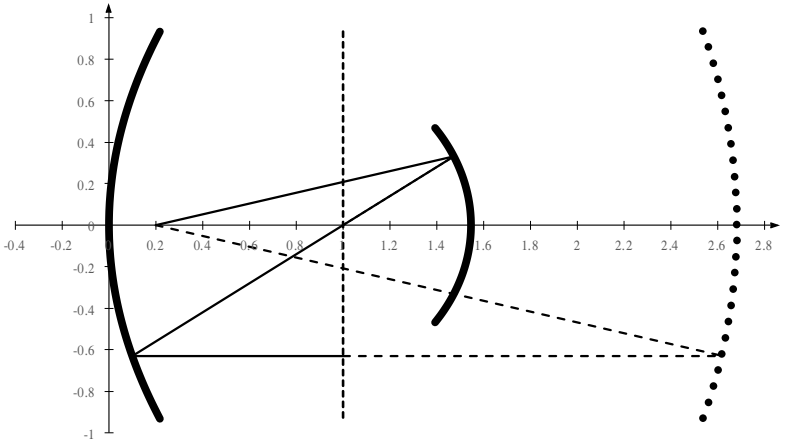


FIGURE 6: The equivalent parabola pertaining to the Gregorian case of Figure 4

In this Figure, the equivalent parabola is shown dotted on the far right. A ray from the feed bounces off the upper part of the sub-reflector then to be reflected again from a point on the lower part of the main reflector and onto a reflection point on the equivalent parabola. Thereafter, in the absence of the sub-reflector it returns to whence it came; if the sub-reflector were present, it would strike it again at a point in the lower half space that was the mirror image (with respect to the axis) of where it struck first in the upper half space.

(d) *Offset reflectors*

The notion of a single offset reflector can be appreciated from Figure 1 where, instead of pointing the axis of the feed energy cone at the centre of the paraboloid, it is aligned to point upwards and illuminate only an offset portion. For a required projected aperture size (usually a system requirement), this results in an increase in the size of the space when compared with the centre-fed system.

In the case of dual reflector systems, it will be apparent from Figures 3 and 4 that the hyperbolic and elliptic sub-reflectors present an area of blockage to some of the energy reflected from the paraboloid. This can be a problem, but there are ways to avoid it if energy from the feed is linearly polarised. For example, the sub-reflector can comprise a grid of suitably thin wires aligned parallel to the polarisation of energy incident from the feed. This energy will be mostly totally reflected and at the main reflector its polarisation can, by proper design, be rotated through ninety degrees on reflection (this is sometimes called a twist reflector or polarisation rotating device), after which the reflected energy will be orthogonal to and transparent to the wire grid sub-reflector, passing through it with very little loss. The details of such matters, however, are beyond the scope of this Article, but the interested reader can gain useful information about such

https://doi.org/10.1017/mag.2021.3 Published online by Cambridge University Press

material by visiting the extensive website [4]. It the reader is not familiar with German, there is an option to select English. Thereafter, select either the *Radar Set (Example given)* option, or *Database of Radars*, whichever appears and select the *Round, covered antennas* picture shown on the page. This will yield a page of photographs with a preamble containing the words *Cassegrain antennas*, which the reader can select for greater appreciation. The feed and its supporting structure will also serve to block the projected aperture, but such effects can be reduced somewhat by allowing for the aperture of the feed (horn) to be flush-mounted at a small central hole in the paraboloid ($d' = 0$) to illuminate the sub-reflector. If it is not possible to circumvent aperture blockage effects using polarisation rotating devices, it is possible to do so in other ways, space permitting. For example, the Gregorian case of Figure 4 lends itself naturally to such a scenario. Taking the upper half of the main reflector and the lower half of the sub-reflector gives Figure 7.

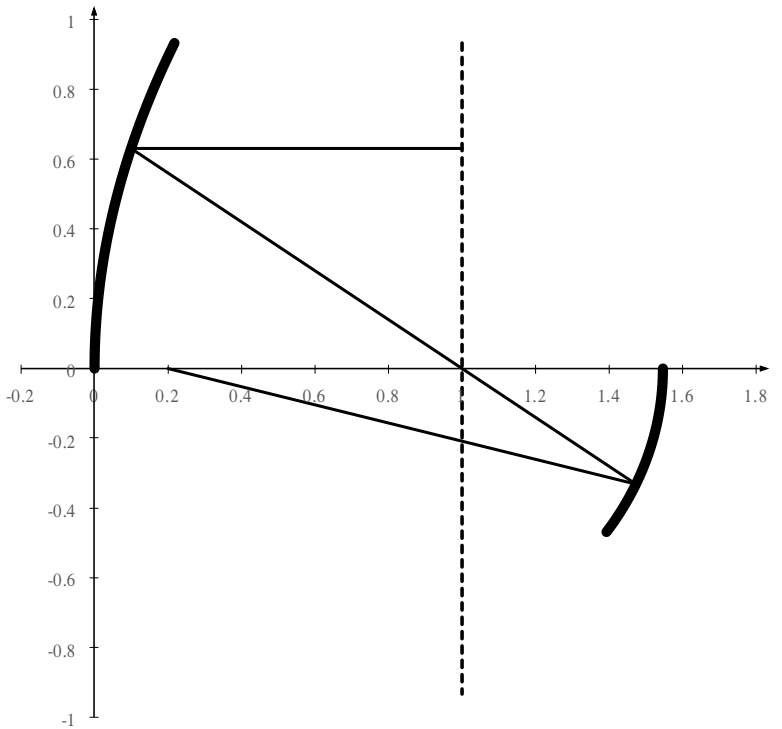


FIGURE 7: An offset geometry for the Gregorian configuration of Figure 4

It can be appreciated from the Figure that the offset sub-reflector portion now presents no blockage to reflection from the offset portion of the paraboloid. It is not a unique scenario. A variety of other offset configurations can be envisaged, even in the Cassegrain case. For example, it will suffice to redesign and repoint a feed horn so that its energy cone

https://doi.org/10.1017/mag.2021.3 Published online by Cambridge University Press

illuminates only that part of the hyperboloid that does not lead to blockage effects, resulting in illumination of an offset portion of the paraboloid at some remove from the origin. Moreover, if the energy cone from the feed is assumed to be right circular then the projected aperture offset shape in the case of the single reflector geometry will be circular [5]. It is left as an exercise for the interested reader to determine, for the above dual offset configurations under such illumination, the ensuing shapes of the projected apertures. An alternative approach is to work backwards and define first the desired shape of the projected aperture (a circular one, say, or indeed an elliptic one) and then ray-trace back to determine the required reflector profiles and the concomitant shape of the energy cone from the feed, and if necessary alter the feed dimensions to suit. It should be appreciated at this point that the design of a feed for a reflector system is a stand-alone subject matter, beyond the scope of this Article.

Finally, it should be realised that in the context of RF engineering, the offset of the real focus in the above classical cases is either positive or zero, but it is not negative, as is the case with some astronomical telescopes. For these, a small central hole can be accommodated in the paraboloid to allow for a negative focus because any such hole would be many millions of wavelengths of light in diameter. In the RF spectrum, wavelengths are significantly longer and such a scenario might not be practical.

Conclusion

A study has been presented to show how the mathematics of conic sections can be employed in the field of RF engineering design to determine and plot reflector shapes in both single and dual reflector systems. No attempt has been made to explain why reflector sizes are what they are, and why the f / d ratio is an important factor from the viewpoint of RF design. It is hoped to address this issue in a future note.

References

1. https://commons.wikimedia.org/wiki/File:Museum_of_Flight_Tornado_01.jpg
2. A. Cockshott and F. B. Walters, *A treatise on geometrical conics*, Macmillan (1943).
3. P. W. Hannan, Microwave antennas derived from the Cassegrain telescope, *IRE Transactions on Antennas and Propagation*, Vol. AP-9, No. 2 (March 1961).
4. radartutorial.eu
5. John Mahony, The cone-paraboloid intercept, *Math. Gaz.* **92** (July 2008) pp. 235-241.

10.1017/mag.2021.3

© The Mathematical Association 2021

JOHN D. MAHONY
5 Bluewater View, Mt. Pleasant, Christchurch 8081, New Zealand
e-mail: *johndmahony@gmail.com*

https://doi.org/10.1017/mag.2021.3 Published online by Cambridge University Press